Anion-Directed Architectures in Amine Halide Peroxosolvates: Role of H_2O_2/H_2O Competition in Crystal Engineering

Andrei V. Churakov,[a] Elena A. Mel'nik,[a] Pavel P. Egorov,[a] Alexey A. Mikhaylov,[a] Tatiana A. Tripol'skaya,[a] Ovadia Lev*[b] and Petr V. Prikhodchenko*[a]

[a] *Kurnakov Institute of General and Inorganic Chemistry, Russian Academy of Sciences, Leninskii prosp. 31, 119991 Moscow, Russia. E-mail: prikhman@gmail.com*

[b] *Casali Center of Applied Chemistry, Hebrew University of Jerusalem, Jerusalem 9190401, Israel. E-mail: ovadia@mail.huji.ac.il*

Table of contents

Materials, synthesis and characterization

1-Adamantanamine hydrochloride (98%), ethylenediamine dihydrochloride (98%), piperazine (98%), triethylenediamine (98%) and hydrogen peroxide (30%) were purchased from Sigma-Aldrich. Piperazine dihydrochloride monohydrate (99%) was purchased from Fisher Scientific.

Glassware for peroxide rich solutions: All glassware were treated by filling with 1M NaOH for 1 day, then with 1M nitric acid for an additional day, and finally with 10% w/w hydrogen peroxide for a further day. Sulfochromic acid or permanganate treatment should be avoided.

Safety note: Concentrating hydrogen peroxide solutions and working with them require safety precautions. Handling procedures for concentrated hydrogen peroxide are described in detail (danger of explosion!).[1–3]

Purification of H_2O_2.

Commercial hydrogen peroxide was concentrated by vacuum distillation. On the first stage, 30% w/w hydrogen peroxide was distilled under vacuum to remove stabilizers and other impurities. The resulting 18-20% w/w pure aqueous hydrogen peroxide was then concentrated under vacuum by passing the argon to obtain 35, 50, 70 and 97% w/w hydrogen peroxide as determined by permanganometry.[2,3]

Hydrogen peroxide with concentrations of 5, 10% w/w and was obtained by diluting of 20% w/w solution with deionized water.

*Synthesis of aminoadamantane hydrochloride peroxosolvates (**1**, **2**)*

Aminoadamantane hydrochloride (0.40 g, 2.1 mmol) was dissolved in 0.6 mL of 97% w/w hydrogen peroxide. Colorless crystals of **1** were obtained by cooling of prepared solution to -20°C for several hours.

Aminoadamantane hydrochloride (0.60 g, 3.2 mmol) was dissolved in 0.6 mL of 50% w/w hydrogen peroxide. Colorless crystals of **2** were obtained by cooling of prepared solution to -20°C for several hours.

*Synthesis of ethylenediammonium dichloride peroxosolvates (**3, 4**).*

Ethylenediamine dihydrochloride (0.74 g, 5.6 mmol) was dissolved in 1 mL of 60% w/w hydrogen peroxide. Colorless crystals of **3** were obtained by cooling of prepared solution to 4°C for several hours. Crystals were filtered and dried. Yield 0.19 g (20%). m.p. = 85°C.

Anal. Calc. for $C_2H_{12}Cl_2N_2O_2$ ***(3)**:* OO (peroxide), 19.16; N, 16.77; C, 14.38; H, 7.24. Found: OO (peroxide), 19.33; N, 16.52; C, 14.37; H, 7.22.

Ethylenediamine dihydrochloride (0.78 g, 5.9 mmol) was dissolved in 1 mL of 50% w/w hydrogen peroxide. Colorless crystals of **4** were obtained by cooling of prepared solution to 4°C for several hours. Crystals were filtered and dried. Yield 0.18 g.

Ethylenediamine dihydrochloride (0.73 g, 5.5 mmol) was dissolved in 1 mL of 45% w/w hydrogen peroxide. Colorless crystals were obtained by cooling of prepared solution to 4°C for several hours. Crystals were filtered and dried. Yield 0.09 g.

*Piperazinium dichloride diperoxosolvate (**5**)*

1.0 g and 1.2 g of piperazine dihydrochloride monohydrate was dissolved in 2 mL of 70 and 97% w/w hydrogen peroxide, respectively. Colorless crystals of 2 were obtained by cooling of prepared solution to 4°C for several hours.

*Piperazinium dichloride monoperoxosolvate (**6-8**)*

1.3 g of piperazine dihydrochloride monohydrate was dissolved in 2 mL of 5, 10, 20, 35 and 50% w/w hydrogen peroxide. Colorless crystals owith different H_2O_2/H_2O ratio were obtained by cooling of prepared solution to 4°C for several hours.

Piperazinium dibromide was prepared from piperazine as previously reported.[4]

*Piperazinium dibromide monoperoxosolvate (**9**)*

0.24 g of piperazine dibromide monohydrate was dissolved in 0.5 mL of 50% w/w hydrogen peroxide. Colorless crystals of 7 were obtained by cooling of prepared solution to 4°C for 30 min.

Additionaly 0.48 g, 0.80 and 0.73 g of piperazine dibromide monohydrate was dissolved in 1 mL of 5, 10 and 35% w/w hydrogen peroxide, respevtively. Colorless crystals of 7 with different H_2O_2/H_2O ratio were obtained by cooling of prepared solution to 4°C for 30 min.

Triethylenediaminium dichloride was prepared from triethylenediamine as previously reported.[5]

*Triethylenediaminium dichloride peroxosolvate (**10**)*

2.0 g of triethylenediaminium dichloride was dissolved in 2 mL of 50% w/whydrogen peroxide. Colorless crystals of **10** were obtained by cooling of prepared solution to 4°C for several hours.

Additionaly, 2 g of triethylenediaminium dichloride was dissolved in 1 mL of 5 and 10% w/w hydrogen peroxide. Colorless crystals of **11** with different H_2O_2/H_2O ratio were obtained by cooling of prepared solution to 4°C for several hours.

X-ray analysis. Absorption corrections based on measurements of equivalent reflections were applied.[6] The structures were solved by direct methods and refined by full matrix least-squares on F^2 with anisotropic thermal parameters for all non-hydrogen atoms.[7] All hydrogen atoms in **3** and **5** were found from difference Fourier synthesis and refined with isotropic thermal parameters. Hydrogen atoms of alkyl groups for **1**, **6, 9-11** were placed in calculated positions and refined using a riding model, while "active" H atoms were found from difference Fourier synthesis, and their positional parameters were refined. In the structures **3**, **7, 8** and **10**, hydrogen peroxide sites are partially occupied by admixed water molecules with occupancies 0.129(7), 0.269(9), 0.617(10) and 0.712(11), respectively. H-atoms of these water molecules were refined with $U_{iso}(H)=1.5\times U_{eq}(O)$. X-ray diffraction studies were performed at the Centre of Shared Equipment of IGIC RAS. Crystal data and details of X-ray analysis are given in Table S1. The crystallographic data for **1-11** have been deposited with the Cambridge Crystallographic Data Centre as supplementary publications under the CCDC numbers 2407244-2407246, 2455698-2455704 and 2489952, respectively.

Elemental analysis. The hydrogen peroxide content in peroxosolvates of chlorides and bromides was determined by permanganometric and iodometric titration, respectively (Table 1).[2] Carbon,

hydrogen and nitrogen content were determined using the vario MICRO cube analyzer (Elementar, Germany).

X-ray powder diffraction. The powder samples were filled into low background quartz sample holders. XRD patterns in the range 10˚ to 60˚ 2θ were recorded at room temperature using CuKα radiation (λ=1.5418 Å) under the following measurement conditions: tube voltage of 40 kV, tube current of 40 mA, step scan mode with a step size 0.02˚ 2θ. XRD patterns were processed by DiffracPlus software.

FTIR spectra were recorded on a JASCO FT/IR-4600 (JASCO, Japan) spectrometer equipped with a diamond ATR accessory.

Differential thermal analysis (DTA) and thermogravimetry analysis (TGA) were performed on simultaneous thermal analyzer, DTG-60 (Shimadzu, Japan). All experiments were carried out under argon flow at a heating rate of 10 °C/min.

Stability study. Samples of compounds **3**, **6** and **10** (approximately 400 mg each) were placed in open glass vials and stored on a laboratory bench at ambient temperature (25 °C) and humidity (ca. 50–60% RH). At predetermined time intervals the peroxode content was determined by permanganometry.

Solid-state DFT calculations.

The space groups and unit cell parameters of **3**, **6**, **9** and **10** obtained in the single-crystal X-ray studies are fixed and structural relaxations are limited to the positional parameters of atoms. The crystal structure of **8** was used to prepare starting geometries for calculation of hydrogen bond energies in pure peroxosolvate **8**-H_2O_2 and hydrate **8**-H_2O of piperazinium chloride by eliminating of water and hydrogen peroxide molecules from scXRD data of **8**, respectively. Density functional theory computations with periodic boundary conditions (solid-state DFT) were performed in the Crystal23 software package[8] using B3LYP functional and the localized basis set 6-31G**. The London dispersion interactions were taken into account by the D3 correction with Becke-Jones damping. The mixing coefficient of Hartree-Fock/Kohn-Sham matrices is set to 25%. Tolerance on energy controlling the self-consistent field convergence for geometry optimizations and frequencies computations is set to 10^{-10} and 10^{-11} Hartree, respectively. The shrinking factor of the reciprocal space net is set to 3. The optimized structures are found to correspond to the minimum point on the potential energy surface.

The Bader analysis of the periodic electron density was performed using Topond21.[9]

The energy of intermolecular H-bonds E_{HB} is evaluated according to ref. [10] as:

$$E_{HB} = 1126 \cdot G_b \qquad \text{(S1)}$$

where G_b is the positively-defined local electronic kinetic energy density at the H···O bond critical point.[11] The Espinosa approach gives reasonable results for energies of intermolecular H-bonds and other non-covalent interactions in organic crystals varying from 2.0 to 50 kJ mol^{-1}.[12]

Supplementary Tables

Table S1. Crystal data and details of X-ray analysis.

	1	**2**	**3**	**4**	**5**
Formula	$C_{20}H_{42}Cl_2N_2O_6$	$C_{20}H_{38}Cl_2N_2O_2$	$C_2H_{12}Cl_2N_2O_2$	$C_2H_{12}Cl_2N_2O_{1.87}$	$C_4H_{16}Cl_2N_2O_4$
*F*w	477.75	409.42	167.04	164.96	227.09
colour, habit	colourless, prism	colourless, prism	colourless, block	colourless, prism	colourless, prism
cryst size (mm)	0.40×0.30×0.20	0.03×0.20×0.05	0.40×0.35×0.30	0.25×0.15×0.10	0.10×0.05×0.05
temperature (K)	100	100	173	100	100
crystal system	monoclinic	triclinic	monoclinic		monoclinic
space group	*P*2/n	$P\bar{1}$	*C*2/*c*	*C*2/*c*	$P2_1/c$
a (Å)	18.7063(9)	6.7122(5)	11.231(2)	11.1837(4)	7.3636(4)
b (Å)	6.3312(3)	11.2178(9)	5.9850(13)	5.9656(2)	11.0879(6)
c (Å)	20.0829(9)	14.5863(12)	11.134(2)	11.0793(4)	6.0534(3)
α (deg)	90	78.253(2)	90	90	90
β (deg)	106.413(2)	78.616(2)	98.835(3)	98.9640(10)	99.808(2)
γ (deg)	90	87.474(3)	90	90	90
V (Å^3)	2281.56(19)	1054.13(14)	739.5(3)	730.15(4)	487.02(4)
Z	4	2	4	4	2
D_c (g·cm^{-3})	1.390	1.290	1.500	1.501	1.549
μ (mm^{-1})	0.324	0.325	0.806	0.814	0.649
F(000)	1032	444	352	348	240
θ range (deg)	1.76 to 29.00	2.57 to 25.24	3.67 to 27.99	3.69 to 30.5	3.36 to 29.00
refl collcd	33522	12068	3160	5774	5409
indep reflns / R_{int}	6053 / 0.077	5064 / 0.020	890 / 0.033	1098 / 0.031	1287 / 0.025
reflns $I>2\sigma(I)$	4801	4473	827	995	1157
No of param	319	265	62	67	87
GooF on F^2	1.022	1.060	1.123	1.175	1.059
R_1 ($I>2\sigma(I)$)	0.0427	0.0396	0.0234	0.0221	0.0197
wR_2(all data)	0.1014	0.1078	0.0669	0.0598	0.0502
largest diff peak / hole (e·Å^{-3})	0.37 / -0.24	0.877 / -0.410	0.27 / -0.20	0.23 / -0.27	0.45 / -0.21

CCDC number	**2407244**	**2407245**	**2407246**	**2455698**	**2455699**

Table S1. (continued)

	6	**7**	**8**	**9**	**10**	**11**
Formula	$C_4H_{14}Cl_2N_2O_2$	$C_4H_{14}Cl_2N_2O_{1.73}$	$C_4H_{14}Cl_2N_2O_{1.38}$	$C_4H_{14}Br_2N_2O_2$	$C_6H_{16}Cl_2N_2O_2$	$C_6H_{16}Cl_2N_2O_{1.29}$
*F*w	193.07	188.75	183.15	281.99	219.11	207.71
colour, habit	colourless, prism	colourless, prism	colourless, prism	colourless, prism	colourless, prism	colourless, prism
cryst size (mm)	0.40×0.30×0.30	0.40×0.30×0.30	0.40×0.30×0.20	0.18×0.12×0.06	0.40×0.30×0.20	0.20×0.15×0.10
temperature (K)	100	100	100	100	100	150
crystal system	monoclinic	monoclinic	monoclinic	monoclinic	monoclinic	monoclinic
space group	*C*2/*c*	*C*2/*c*	*C*2/*c*	*C*2/*c*	*C*2/*c*	*C*2/*c*
a (Å)	10.7011(9)	10.6313(7)	10.479(1)	11.1916(9)	9.7834(6)	9.7389(8)
b (Å)	6.1485(7)	6.1567(4)	6.1798(6)	6.2618(5)	9.3257(6)	9.5339(8)
c (Å)	13.6061(15)	13.5716(12)	13.5150(16)	13.9442(12)	10.6627(7)	10.3448(9)
α (deg)	90	90	90	90	90	90
β (deg)	111.074(3)	110.665(2)	109.635(3)	111.211(3)	98.935(2)	99.768(3)
γ (deg)	90	90	90	90	90	90
V (Å^3)	835.35(15)	831.16(11)	824.31(15)	911.00(13)	961.03(11)	946.59(14)
Z	4	4	4	4	4	4
D_c (g·cm^{-3})	1.535	1.508	1.476	2.056	1.514	1.457
μ (mm^{-1})	0.725	0.725	0.725	8.851	0.641	0.641
F(000)	408	399	388	552	464	441
θ range (deg)	3.21 to 30.52	3.21 to 30.54	3.20 to 28.00	3.13 to 25.24	3.04 to 25.24	3.01 to 25.24
refl collcd	4720	7820	5877	6168	6400	7093
indep reflns / R_{int}	1120 / 0.039	1277 / 0.033	993 / 0.039	1211 / 0.050	1277 / 0.048	1260 / 0.037
reflns $I>2\sigma(I)$	980	1184	884	1093	1132	1140
No of param	58	67	66	58	63	72
GooF on F^2	1.039	1.117	1.140	1.165	1.044	1.051
R_1 ($I>2\sigma(I)$)	0.0297	0.0224	0.0251	0.0231	0.0297	0.0265
wR_2(all data)	0.0634	0.0528	0.0567	0.0570	0.0718	0.0666
largest diff peak / hole (e·Å^{-3})	0.48 / -0.27	0.40 / -0.24	0.39 / -0.22	0.43 / -0.72	0.38 / -0.35	0.42 / -0.20
CCDC number	**2455700**	**2455701**	**2455702**	**2455703**	**2455704**	**2489952**

Table S2. Hydrogen-bond geometry in **1** (Å, °).

D—H···*A*	*D*—H	H···*A*	*D*···*A*	*D*—H···*A*
O(1)—H(1)···Cl(1)^{i}	0.82(2)	2.32(2)	3.1207(13)	166(2)
O(2)—H(2)···O(4)	0.89(2)	1.91(2)	2.7974(17)	172(2)
O(3)—H(3)···Cl(2)	0.84(2)	2.18(2)	3.0164(13)	174(2)
O(4)—H(4)···Cl(1)	0.82(2)	2.22(2)	3.0359(13)	173(2)
O(5)—H(5)···O(3)	0.85(3)	1.95(3)	2.7905(17)	172(2)
O(6)—H(6)···Cl(2)^{ii}	0.87(3)	2.20(3)	3.0537(13)	170(2)
N(1)—H(13)···O(1)	0.92(2)	2.08(2)	2.9699(19)	160.8(18)
N(2)—H(21)···O(6)	0.90(2)	2.14(2)	2.9794(19)	154.9(19)
N(1)—H(11)···Cl(2)	0.84(2)	2.39(2)	3.2054(15)	164.2(18)
N(2)—H(22)···Cl(1)	0.91(2)	2.30(3)	3.2043(15)	174(2)

Symmetry codes: (i) −*x*+3/2, *y*−1, −*z*+3/2; (ii) −*x*+1, −*y*+2, −*z*+1.

Table S3. Hydrogen bond geometry in **2** (Å, °).

D—H···*A*	*D*—H	H···*A*	*D*···*A*	*D*—H···*A*
O(1)—H(1)···Cl(2)	0.97(2)	2.12(2)	3.0863(14)	172(2)
O(2)—H(2)···Cl(1)	1.02(2)	2.15(2)	3.0998(14)	154(2)
N(1)—H(11)···Cl(1)	0.87(2)	2.40(2)	3.2606(15)	171(2)
N(1)—H(12)···Cl(1)^{i}	0.87(2)	2.47(2)	3.1906(15)	141(2)
N(1)—H(13)···Cl(2)	0.90(2)	2.27(2)	3.1665(15)	178(2)
N(2)—H(22)···Cl(1)^{ii}	0.91(3)	2.34(3)	3.2499(16)	175(2)
N(2)—H(23)···O(1)	0.92(2)	2.05(2)	2.8199(19)	140(2)
N(2)—H(21)···Cl2^{iii}	0.92(3)	2.23(3)	3.1303(15)	165 (2)

Symmetry codes: (i) −*x*+1, −*y*+1, −*z*+1; (ii) −*x*+2, −*y*+1, −*z*+1; (iii) *x*+1, *y*, *z*.

Table S4. Hydrogen bond geometry in **3** (Å, °).

D—H···*A*	*D*—H	H···*A*	*D*···*A*	*D*—H···*A*
O(1)—H(1)···Cl(1)	0.92(2)	2.23(2)	3.1445(12)	175.7(18)
N(1)—H(11)···Cl(1)	0.865(18)	2.376(17)	3.1866(12)	156.2(14)
N(1)—H(12)···Cl(1)^{i}	0.895(18)	2.594(17)	3.2557(13)	131.4(13)
N(1)—H(12)···Cl(1)^{ii}	0.895(18)	2.821(17)	3.3832(13)	122.1(13)
N(1)—H(13)···Cl(1)^{iii}	0.871(18)	2.329(18)	3.1866(13)	168.1(15)

Symmetry codes: (i) *x*−1/2, *y*−1/2, *z*; (ii) −*x*+1/2, −*y*+3/2, −*z*+1; (iii) −*x*+1/2, *y*−1/2, −*z*+1/2.

Table S5. Hydrogen bond geometry in **4** (Å, °).

D—H···*A*	*D*—H	H···*A*	*D*···*A*	*D*—H···*A*
O(1)—H(1)···Cl(1)	0.88(2)	2.26(2)	3.1322(12)	172(2)
O(2)—H(2)···Cl(1)	0.88	2.70	3.364(8)	133
N(1)—H(13)···Cl(1)	0.897(17)	2.334(16)	3.1749(10)	156.2(13)
N(1)—H(11)···Cl(1)^{i}	0.903(17)	2.576(17)	3.2429(10)	131.2(13)
N(1)—H(11)···Cl(1)^{ii}	0.903(17)	2.788(16)	3.3626(10)	122.6(12)
N(1)—H(12)···Cl(1)^{iii}	0.886(16)	2.321(16)	3.1812(10)	163.6(14)

Symmetry codes: (i) *x*−1/2, *y*−1/2, *z*; (ii) −*x*+1/2, −*y*+3/2, −*z*+1; (iii) −*x*+1/2, *y*−1/2, −*z*+1/2.

Table S6. Hydrogen-bond geometry in **5** (Å,°).

D—H···*A*	*D*—H	H···*A*	*D*···*A*	*D*—H···*A*
O(1)—H(1)···Cl(1)	0.837(16)	2.262(16)	3.0947(8)	173.4(14)
O(2)—H(2)···Cl(1)^{i}	0.820(16)	2.481(16)	3.2377(8)	154.0(14)
N(1)—H(4)···Cl(1)^{i}	0.897(15)	2.401(15)	3.1830(8)	145.8(12)
N(1)—H(3)···Cl(1)^{ii}	0.868(14)	2.318(14)	3.1672(8)	165.9(12)

Symmetry codes: (i) −x+1, −*y*+1, −*z*; (ii) −*x*+1, −*y*+1, −*z*+1.

Table S7. Hydrogen-bond geometry in **6** (Å, °).

D—H···*A*	*D*—H	H···*A*	*D*···*A*	*D*—H···*A*
N(1)—H(12)···O(1)	0.88(2)	2.29(2)	2.9419(18)	131.4(16)
O(1)—H(1)···Cl(1)^{i}	0.86(2)	2.29(3)	3.1342(13)	167(2)
N(1)—H(11)···Cl(1)	0.890(18)	2.325(19)	3.1633(14)	156.9(16)
N(1)—H(12)···Cl(1)^{ii}	0.88(2)	2.56(2)	3.2223(14)	132.6(16)

Symmetry codes: (i) −*x*+1, *y*−1, −*z*+3/2; (ii) *x*+1/2, *y*−1/2, *z*.

Table S8. Hydrogen bonds geometry in **7** and **8** (Å, °).

D—H···*A*	*D*—H	H···*A*	*D*···*A*	*D*—H···*A*
7				
N(1)—H(12)···Cl(1)	0.892(15)	2.312(15)	3.1592(9)	158.6(13)
N(1)—H(11)···Cl(1)^{i}	0.908(15)	2.489(15)	3.2001(9)	135.5(12)
N(1)—H(11)···O(1)	0.908(15)	2.285(15)	2.9398(16)	128.8(12)
N(1)—H(11)···O(2)	0.908(15)	2.674(15)	3.211(4)	118.8(11)
O(1)—H(1)···Cl(1)^{ii}	0.85(3)	2.29(3)	3.1257(15)	169(3)
O(2)—H(2)···Cl(1)^{ii}	0.85(2)	2.62(7)	3.367(4)	147(10)
8				
N(1)—H(12)···Cl(1)	0.938(19)	2.244(19)	3.1455(14)	161.0(15)
N(1)—H(11)···Cl(1)^{i}	0.872(19)	2.453(19)	3.1639(13)	139.1(16)
N(1)—H(11)···O(1)	0.872(19)	2.338(19)	2.944(4)	126.7(15)
N(1)—H(11)···O(2)	0.872(19)	2.700(19)	3.190(3)	116.8(14)
O(1)—H(1)···Cl(1)^{ii}	0.84(2)	2.31(3)	3.118(4)	161(5)
O(2)—H(2)···Cl(1)^{ii}	0.84(2)	2.61(3)	3.379(3)	155(5)

Symmetry codes: (i) *x*+1/2, *y*−1/2, *z*; (ii) −*x*+1, *y*−1, −*z*+3/2.

Table S9. Hydrogen-bond geometry in **9** (Å, °).

D—H···*A*	*D*—H	H···*A*	*D*···*A*	*D*—H···*A*
N(1)—H(12)···O(1)	0.93(3)	2.29(3)	2.964(3)	128.2(2)
O(1)—H(1)···Br(1)^{i}	0.92(4)	2.45(4)	3.3173(19)	158(3)
N(1)—H(11)···Br(1)	0.93(3)	2.41(3)	3.304(2)	160(2)
N(1)—H(12)···Br(1)^{ii}	0.93(3)	2.62(3)	3.334(2)	134(2)

Symmetry codes: (i) −*x*+1, *y*−1, −*z*+1/2; (ii) *x*-1/2, *y*−1/2, *z*.

Table S10. Hydrogen bonds geometry in **10** (Å, °).

D—H···*A*	*D*—H	H···*A*	*D*···*A*	*D*—H···*A*
O(1)—H(1)···Cl(1)	0.87(3)	2.25(3)	3.1160(14)	173(2)
N(1)—H(11)···Cl(1)	0.93(2)	2.24(2)	3.0878(13)	151.7(17)

Table S11. Hydrogen bonds geometry in **11** (Å, °).

D—H···*A*	*D*—H	H···*A*	*D*···*A*	*D*—H···*A*
O(1)—H(1)···Cl(1)	0.81(4)	2.19(4)	2.993(6)	172(10)
O(2)—H(2)···Cl(1)	0.80(4)	2.57(4)	3.349(1)	165(5)
N(1)—H(3)···Cl(1)	0.925(17)	2.244(17)	3.073(1)	148(2)

Table S12. Optimized parameters of the D-H…A (D=O, N; A=O, Cl) H-bonds and computed values of the electron density, ρ_b, the local electronic kinetic energy density, G_b at the hydrogen bonds critical point and the energy values E_{HB} in **3**.

Fragment	d(D…A), Å	d(H…A), Å	∠(D-H…A), °	ρ_b, a.u.	G_b a.u.	E_{HB}[a] kJ mol^{-1}
O(1)—H(1)···Cl(1)	3.143	2.167	170	0.0272	0.0168	18.9
N(1)—H(11)···Cl(1)	3.181	2.227	152	0.0248	0.0161	18.1
N(1)—H(12)···Cl(1)^{i}	3.265	2.503	130	0.0141	0.0103	11.6
N(1)—H(12)···Cl(1)^{ii}	3.352	2.250	176	-	-	-
N(1)—H(13)···Cl(1)^{iii}	3.175	2.159	165	0.0287	0.0177	20.0
N(1)^{iv}-H(12)^{iv}···O(1)	2.837	2.458	101	0.0111	0.0099	11.2
C(1)-H(22)···O(1)	3.732	2.671	164	0.0065	0.0048	5.4
C(1)^{v}-H(21)^{v}···O(1)	3.529	2.463	165.5	0.0098	0.0070	7.9
C(1)^{vi}-H(22)^{vi}…Cl(1)	3.485	2.980	109	0.0069	0.0048	5.4

[a] Eq. S1; Symmetry codes: (i) $x-1/2, y-1/2, z$; (ii) $-x+1/2, -y+3/2, -z+1$; (iii) $-x+1/2, y-1/2, -z+1/2$; (iv) $x+1/2, y-1/2, z$; (v) $x+1/2, y+1/2, z$; (vi) $x, y+1/2, z$.

Table S13. Optimized parameters of the D-H…A (D=O, N; A=O, Cl) H-bonds and computed values of the electron density, ρ_b, the local electronic kinetic energy density, G_b at the hydrogen bonds critical point and the energy values E_{HB} in **6**.

Fragment	d(D…A), Å	d(H…A), Å	∠(D-H…A), °	ρ_b, a.u.	G_b a.u.	E_{HB}[a] kJ mol^{-1}
N(1)—H(12)···O(1)	2.929	2.163	129	0.0166	0.0134	15.1
O(1)—H(1)···Cl(1)^{i}	3.163	2.201	165	0.0254	0.0157	17.7
N(1)—H(11)···Cl(1)	3.169	2.186	157	0.0273	0.0171	19.3
N(1)—H(12)···Cl(1)^{ii}	3.233	2.430	134	0.0162	0.0117	13.2
C(1)—H(112)···Cl(1)^{iii}	3.443	2.883	112	0.0083	0.0059	6.6
C(1)—H(111)···Cl(1)^{vi}	3.4612	2.676	129	0.0113	0.0080	9.0
C(2)—H(212)···O(1)^{v}	3.504	2.694	131	0.0063	0.0048	5.4
C(2)—H(212)···Cl(1)^{vi}	3.675	2.950	124	0.0066	0.0043	4.9
C(1)—H(112)···Cl(1)^{vii}	3.550	2.712	133	0.0106	0.0073	8.2
C(2)—H(211)···Cl(1)^{viii}	3.597	3.025	113	0.0061	0.0040	4.5

Symmetry codes: (i) −*x*+1, *y*−1, −*z*+3/2; (ii) *x*+1/2, *y*−1/2, *z*; (iii) −*x*+1, *y*, −*z*+3/2; (iv) −*x*+1/2, *y*−1/2, −*z*+3/2; (v) −*x*+1, −*y*+1, −*z*+1; (vi) −*x*+1, −*y*+2, −*z*+1; (vii) *x*+1/2, *y*+1/2, *z*; (vii) −*x*+1/2, −*y*+3/2, *z*;

Table S14. Optimized parameters of the D-H…A (D=O, N; A=O, Cl) H-bonds and computed values of the electron density, ρ_b, the local electronic kinetic energy density, G_b at the hydrogen bonds critical point and the energy values E_{HB} in **9**.

Fragment	d(D…A), Å	d(H…A), Å	∠(D-H…A), °	ρ_b, a.u.	G_b a.u.	E_{HB}[a)] kJ mol^{-1}
N(1)—H(12)···O(1)	2.975	2.235	127	0.0144	0.0117	13.2
O(1)—H(1)···Br(1)^{i}	3.299	2.335	165	0.0238	0.0129	14.5
N(1)—H(11)···Br(1)	3.298	2.309	158	0.0258	0.0143	16.1
N(1)—H(12)···Br(1)^{ii}	3.351	2.553	134	0.0157	0.0099	11.2
C(2)—H(212)···O(1)^{iii}	3.671	2.890	129	0.0063	0.0048	5.4
C(2)—H(212)···Br(1)^{iv}	3.571	2.979	115	0.0086	0.0055	6.2
C(2)—H(212)···Br(1)^{v}	3.570	2.779	129	0.0115	0.0072	8.1
C(2)—H(212)···Br(1)^{vi}	3.676	2.825	135	0.0041	0.0031	3.5

Symmetry codes: (i) −*x*+1, *y*−1, −*z*+1/2; (ii) *x*−1/2, *y*−1/2, *z*; (iii) −*x*+1, *y*, −*z*+3/2; (iv) *x*−1/2, *y*+1/2, *z*; (v) −*x*+1, *y*, −*z*+1/2; (vi) −*x*+1, −*y*+1, −*z*+1.

Table S15. Optimized parameters of the D-H…A (D=O, N; A=O, Cl) H-bonds and computed values of the electron density, ρ_b, the local electronic kinetic energy density, G_b at the hydrogen bonds critical point and the energy values E_{HB} in **10**.

Fragment[a)]	d(D…A), Å	d(H…A), Å	∠(O-H…A), °	ρ_b, a.u.	G_b a.u.	E_{HB}[a)] kJ mol^{-1}
O(1)—H(1)···Cl(1)	3.145	2.162	174	0.0274	0.0166	18.7
N(1)—H(11)···Cl(1)	3.1126	2.165	150	0.0287	0.0179	20.2
C(1)—H(112)···O(1)^{i}	3.196	2.628	112	0.0081	0.0064	7.2
C(2)^{ii}—H(212)^{ii}···O(1)	3.290	2.261	165	0.0151	0.0113	12.7
C(1)—H(111)···Cl(1)^{iii}	3.579	2.623	145	0.0118	0.0081	9.1
C(2)—H(211)···Cl(1)^{iv}	3.414	2.652	127	0.0116	0.0083	9.3
C(2)—H(211)···Cl(1)^{v}	3.591	2.960	117	0.0083	0.0056	6.3
C(3)—H(312)···Cl(1)^{v}	3.612	2.840	128	0.0070	0.0046	5.2

Symmetry codes: (i) −*x*+1/2, *y*,*z*; (ii) −*x*, *y*, −*z*+1/2; (iii) *x*, −*y*+1, *z*−1/2; (iv) −*x*+1/2, *y*+1/2, −*z*+1/2; (v) −*x*+1/2, −*y*+3/2, −*z*+1.

Table S16. Optimized parameters of the D-H…A (D=O, N; A=O, Cl) H-bonds and computed values of the electron density, ρ_b, the local electronic kinetic energy density, G_b at the hydrogen bonds critical point and the energy values E_{HB} in **8**-H_2O_2 and **8**-H_2O.

Fragment	d(D…A), Å	d(H…A), Å	∠(D-H…A), °	ρ_b, a.u.	G_b a.u.	E_{HB}[a] kJ mol^{-1}
8-H_2O_2						
N(1)—H(12)···O(1)	2.914	2.160	128	0.0168	0.0137	15.4
O(1)—H(1)···Cl(1)^{i}	3.165	2.209	164	0.0249	0.0155	17.5
C(2)—H(212)···O(1)^{ii}	3.504	2.694	108	0.0067	0.0050	5.7
8-H_2O						
N(1)—H(12)···O(1)	3.168	2.668	110	0.0067	0.0059	6.6
O(1)—H(1)···Cl(1)^{i}	3.342	2.435	155	0.0157	0.0104	11.7

Symmetry codes: (i) $-x+1, y-1, -z+3/2$; (ii) $-x+1, -y+1, -z+1$.

Supplementary Figures

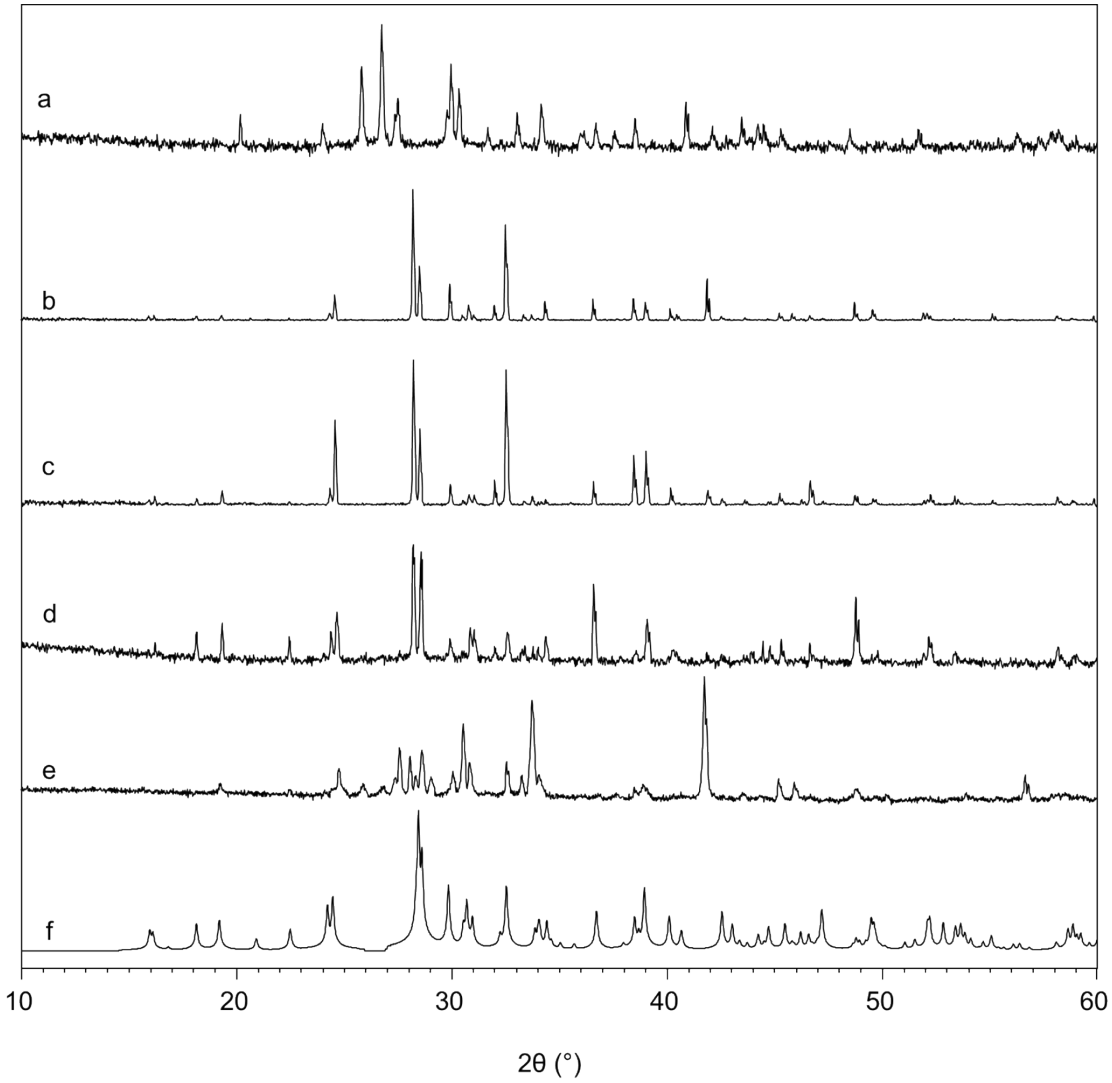

Figure S1. Powder X-Ray diffractogram of ethylenediammonium dichloride (a), ethylenediammonium dichloride peroxosolvates obtained from 97 (b), 80 (c), 60 (**3**, d) and 50 H_2O_2 wt% (**4**, e), and calculated from scXRD data for **3** (f) .

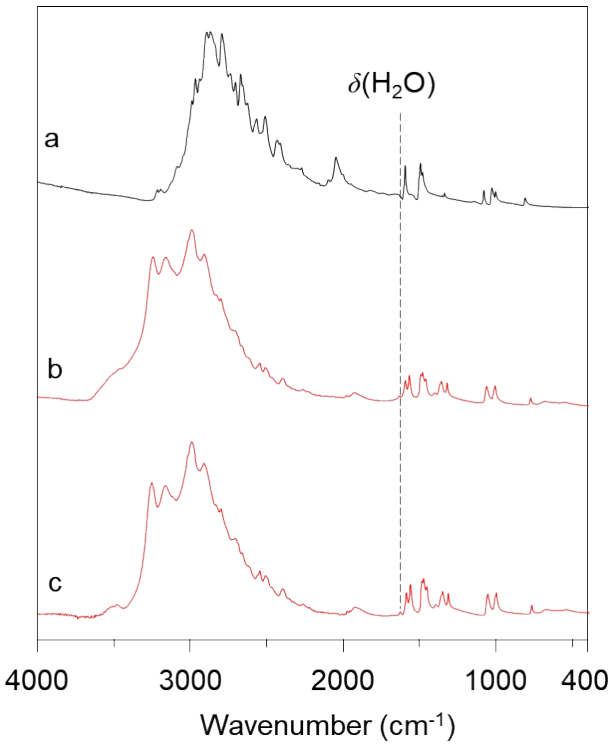

Figure S2. FTIR spectra of ethylenediammonium dichloride (a) and ethylenediammonium dichloride peroxosolvates obtained from 60 (**3**, b) and 50% w/w H_2O_2 (**4**, c), respectively.

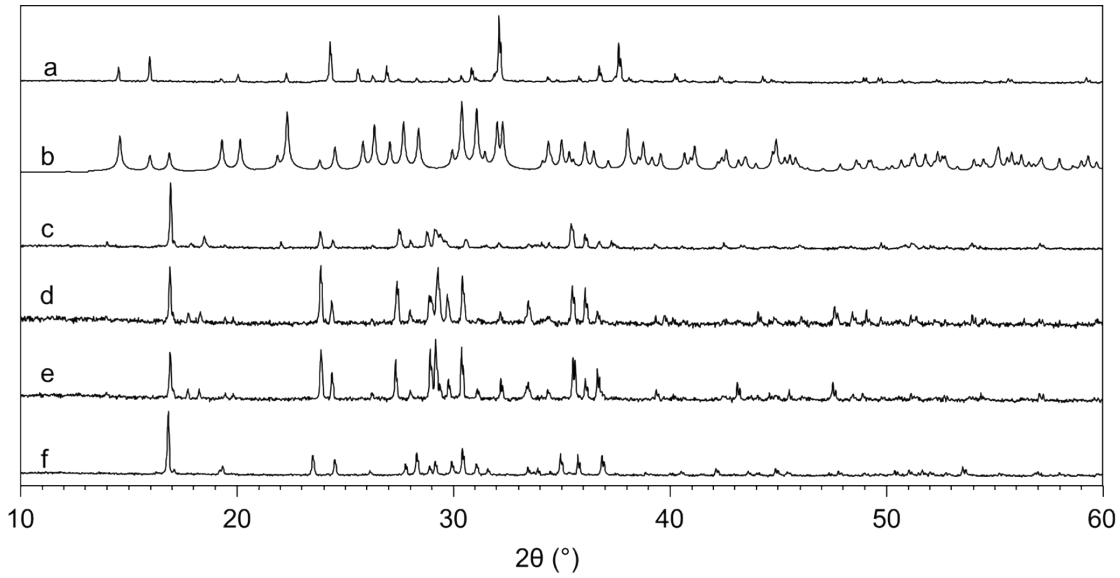

Figure S3. Powder X-ray diffractogram of piperazinium dichloride diperoxosolvate **5** obtained from 97% w/w (a) and its theoretical diffractogram (b), piperazinium dichloride monoperoxosolvates obtained from 10 (c), 20 (d) and 50% w/w H_2O_2 (e) and piperazinium dichloride monohydrate (f).

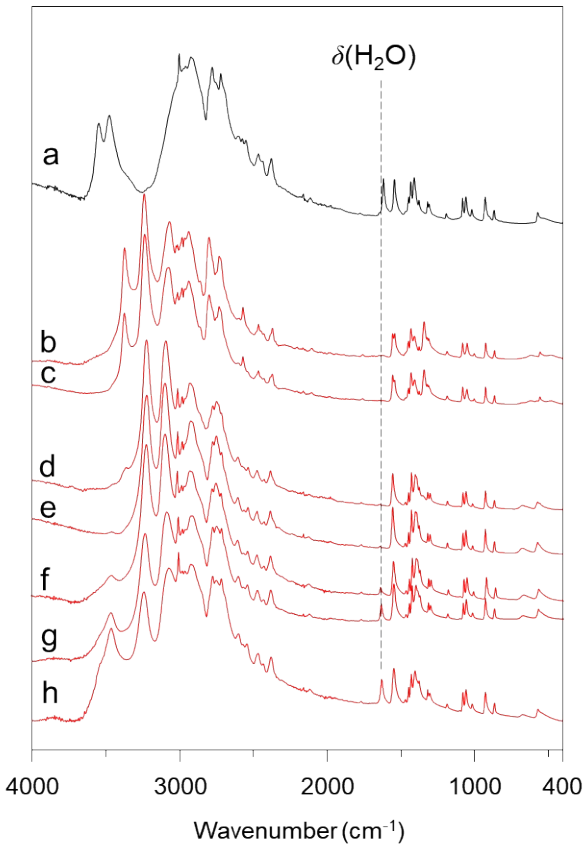

Figure S4. FTIR spectra of piperazinium dichloride monohydrate (a), piperazinium dichloride diperoxosolvate (**5**) obtained from 97 (b) and 70% w/w H_2O_2 (c), piperazinium dichloride monoperoxosolvate (**6**) obtained from 50 (d) and 35 (e), 20 (f), 10 (**7**, g) and 5% w/w H_2O_2 (**8**, h).

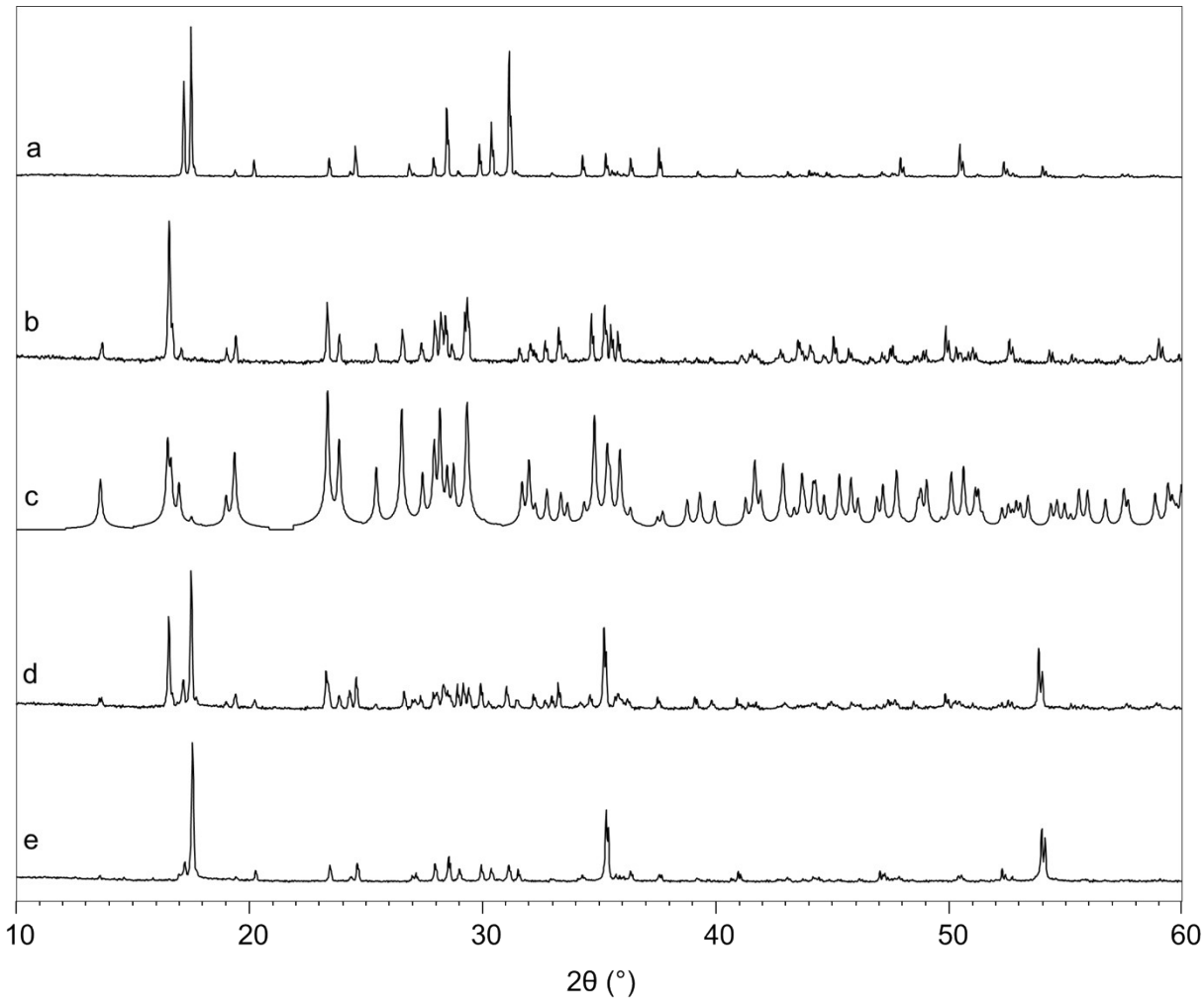

Figure S5. Powder XRD of piperazinium dibromide monohydrate (a), piperazinium dibromide monoperoxosolvate (**9**) obtained from 35 (b), 10 (d), 5% w/w (e) and theoretical diffractogram of piperazinium dibromide monoperoxosolvate (c).

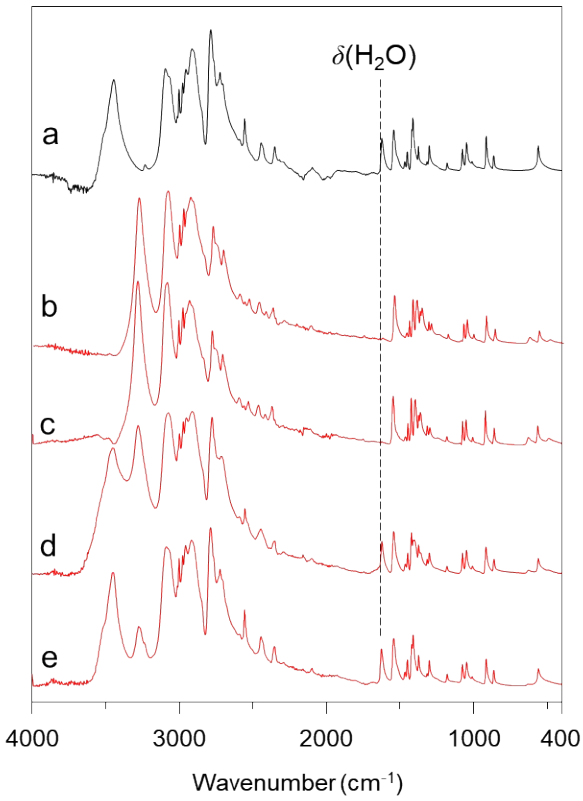

Figure S6. FTIR spectra of piperazinium dibromide monohydrate (a), piperazinium dibromide monoperoxosolvate (**9**) obtained from 50 (b), 35 (c), 10 (d) and 5% w/w H_2O_2 (e).

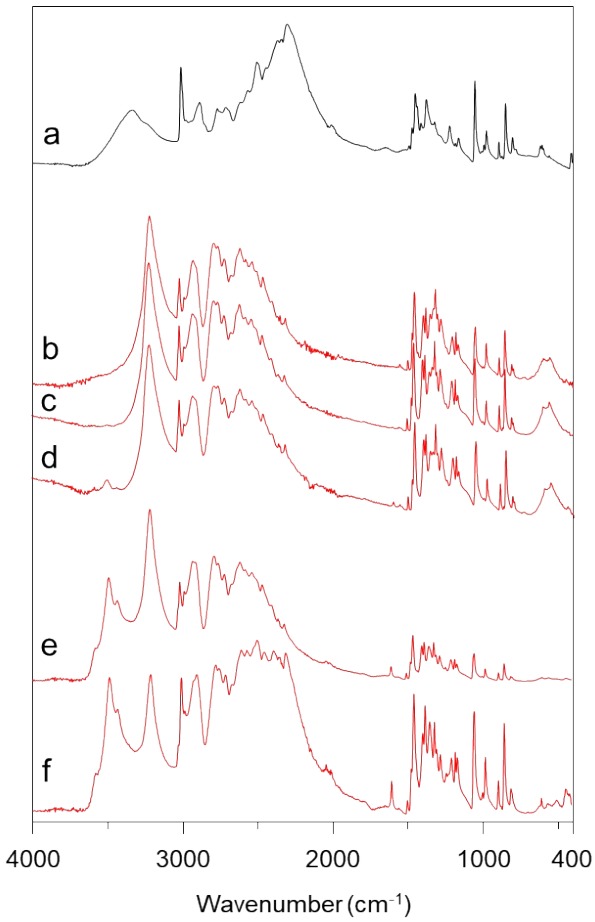

Figure S7. FTIR spectra of triethylenediaminium dichloride (a) and triethylenediaminium dichloride recrystallized from 50 (**10**, b), 35 (c), 20 (d), 10 (e) and 5% w/w H_2O_2 (f).

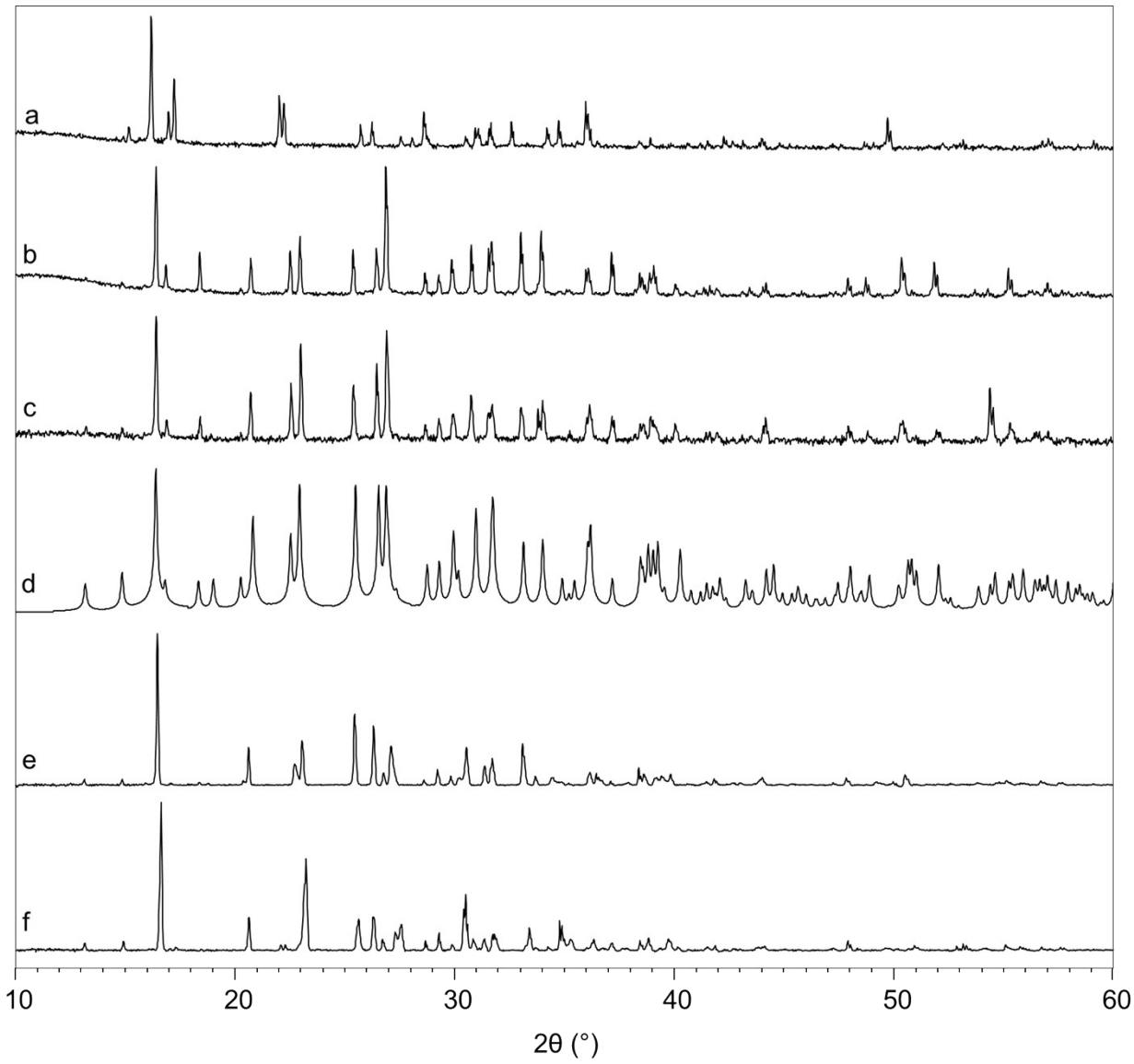

Figure S8. Powder XRD of triethylenediaminium dichloride (a) and its solvates obtained from 50 (b), 20 (c), 10 (e), 5% w/w H_2O_2 (f) and theoretical diffractogram of triethylenediaminium dichloride peroxosolvate (d).

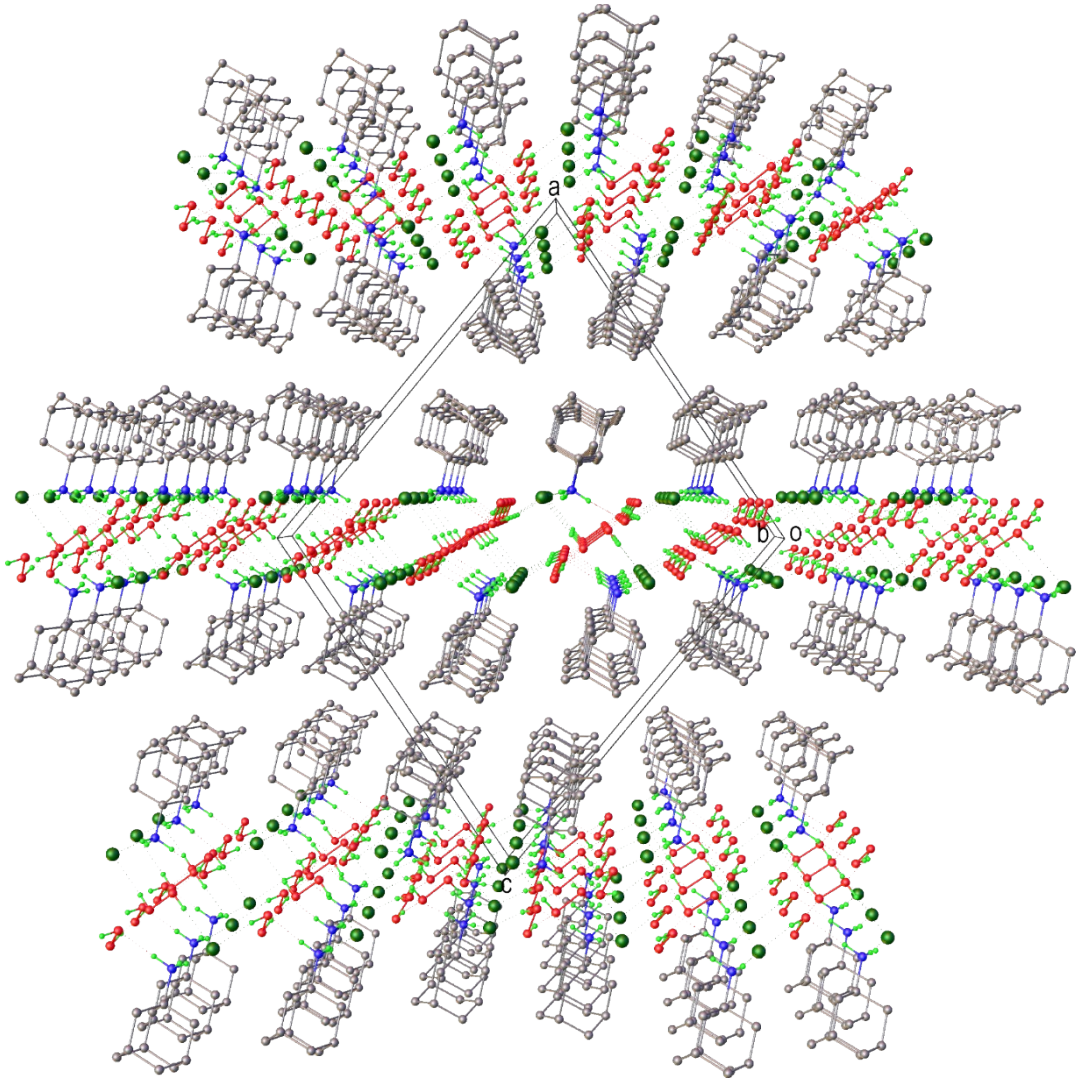

Figure S9. Crystal packing in the crystal structure of **1.** H atoms of alkyl fragments are omitted for clarity. Hydrogen bonds are shown by dashed lines.

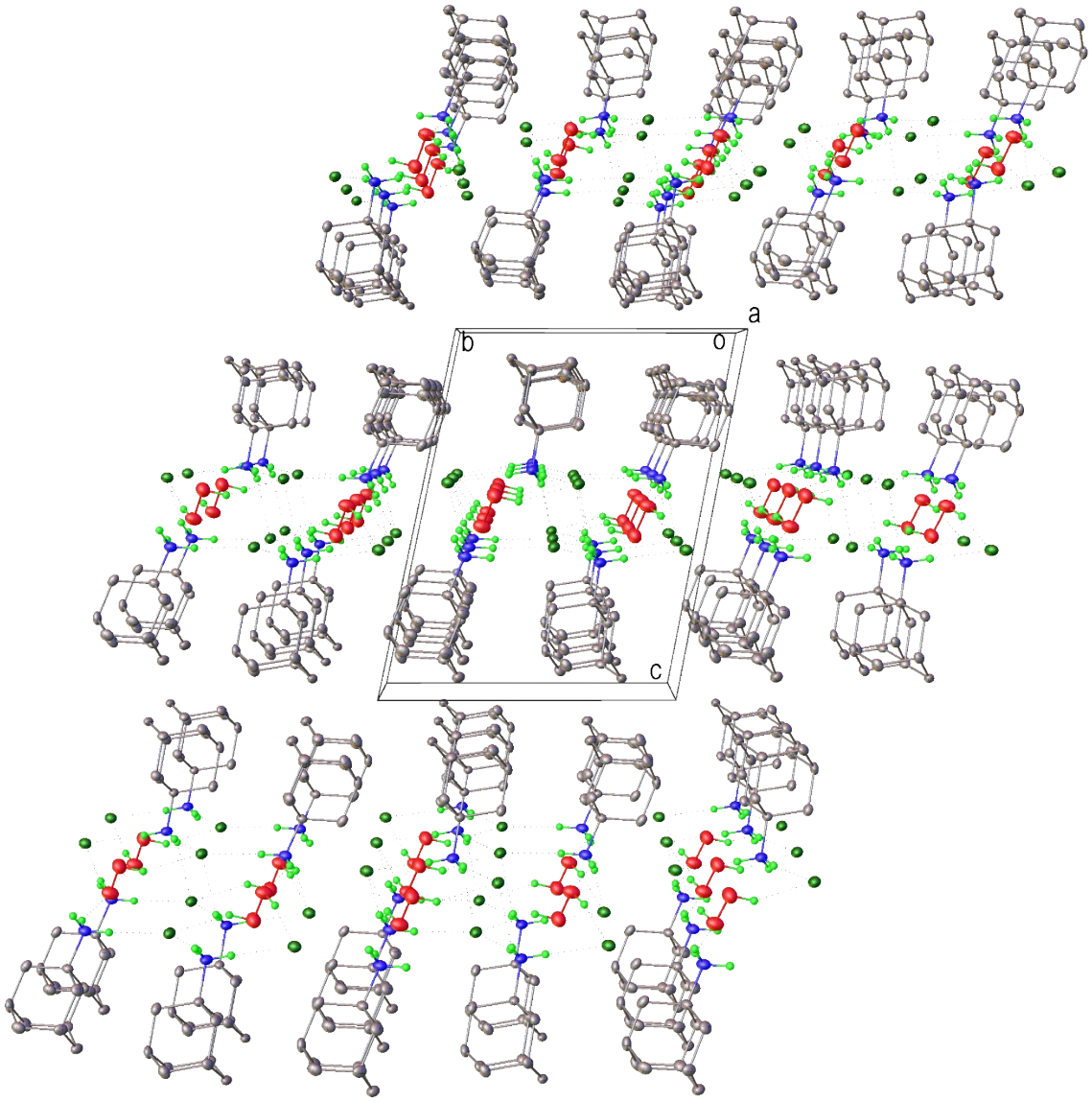

Figure S10. Crystal packing in the crystal structure of **2**. H atoms of alkyl fragments are omitted for clarity. Hydrogen bonds are shown by dashed lines.

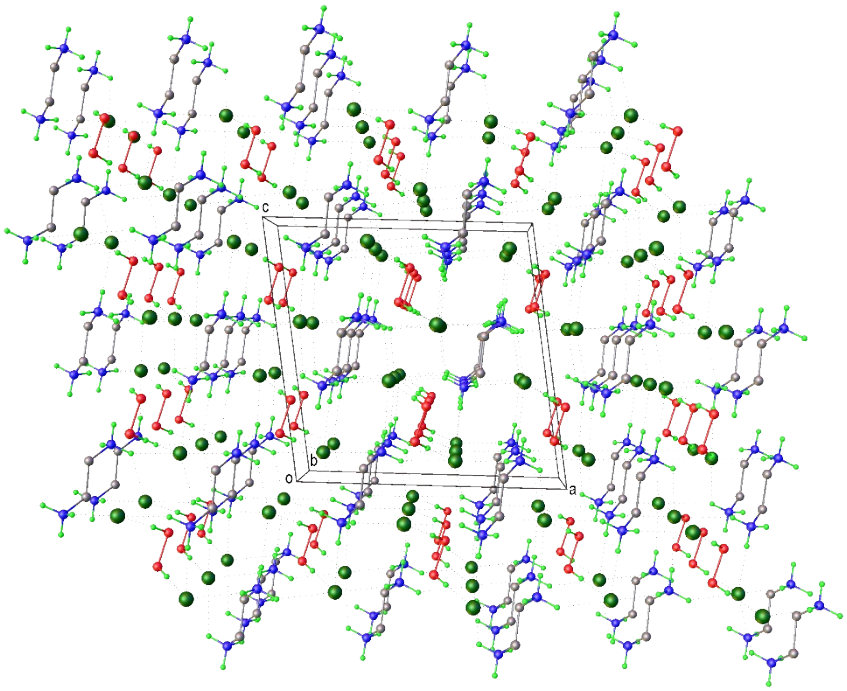

Figure S11. Crystal packing in the crystal structure of **3**. H atoms of alkyl fragments are omitted for clarity. Hydrogen bonds are shown by dashed lines.

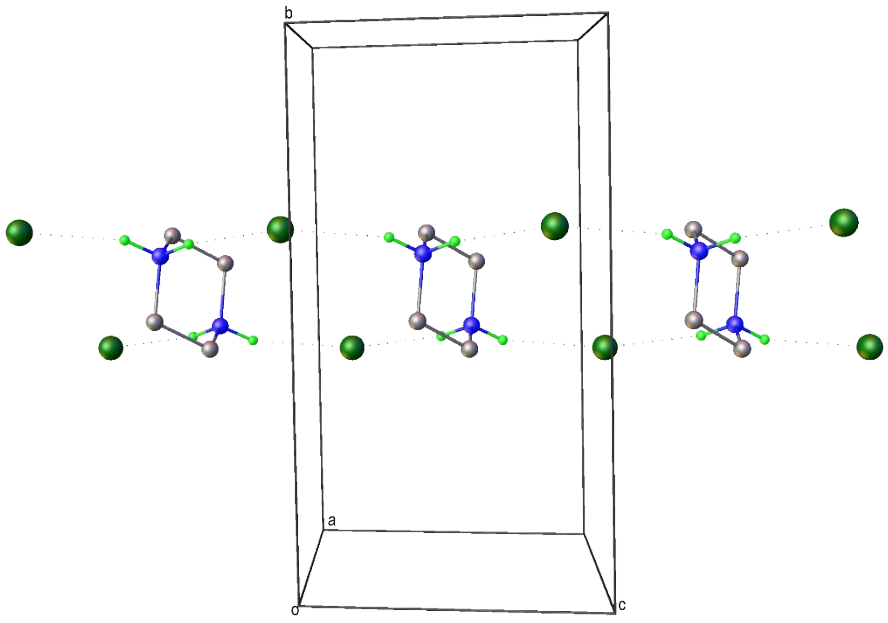

Figure S12. Hydrogen-bonded chains in **5**. H atoms of alkyl fragments are omitted for clarity. Hydrogen bonds are shown by dashed lines.

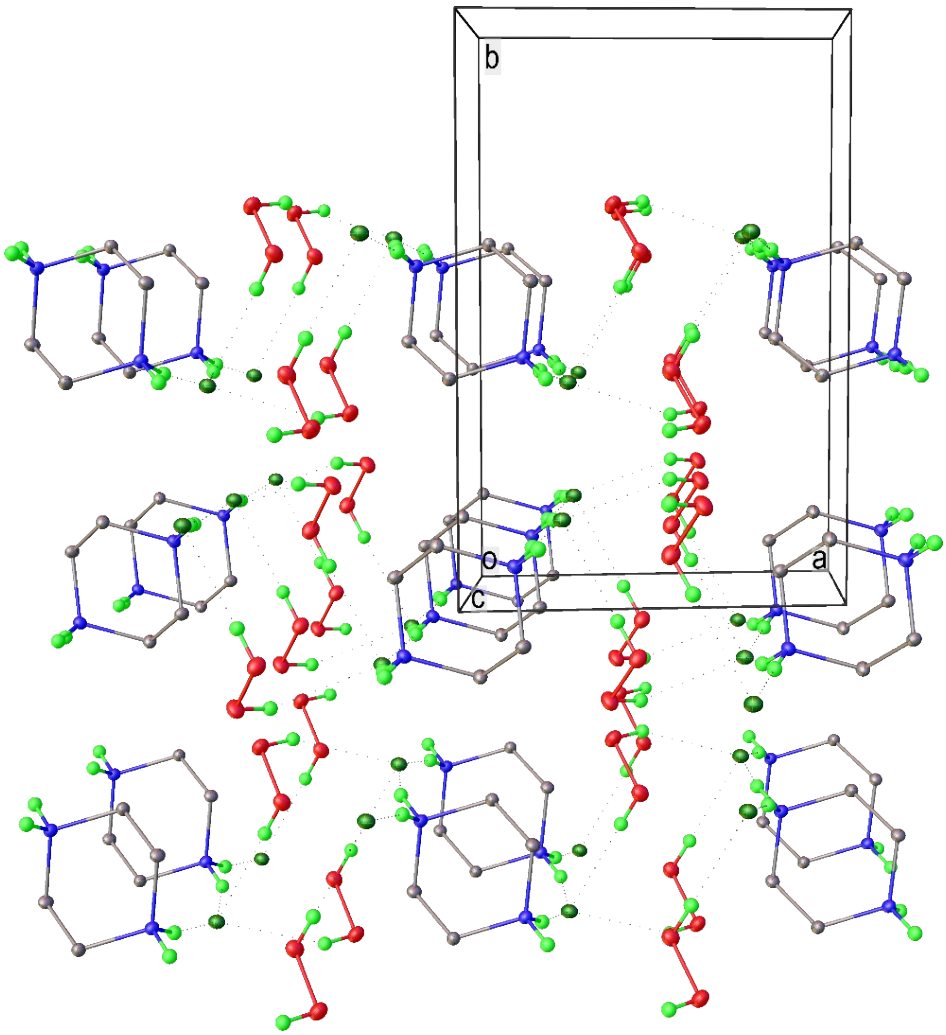

Figure S13. Crystal packing in **5**. H atoms of alkyl fragments are omitted for clarity. Hydrogen bonds are shown by dashed lines.

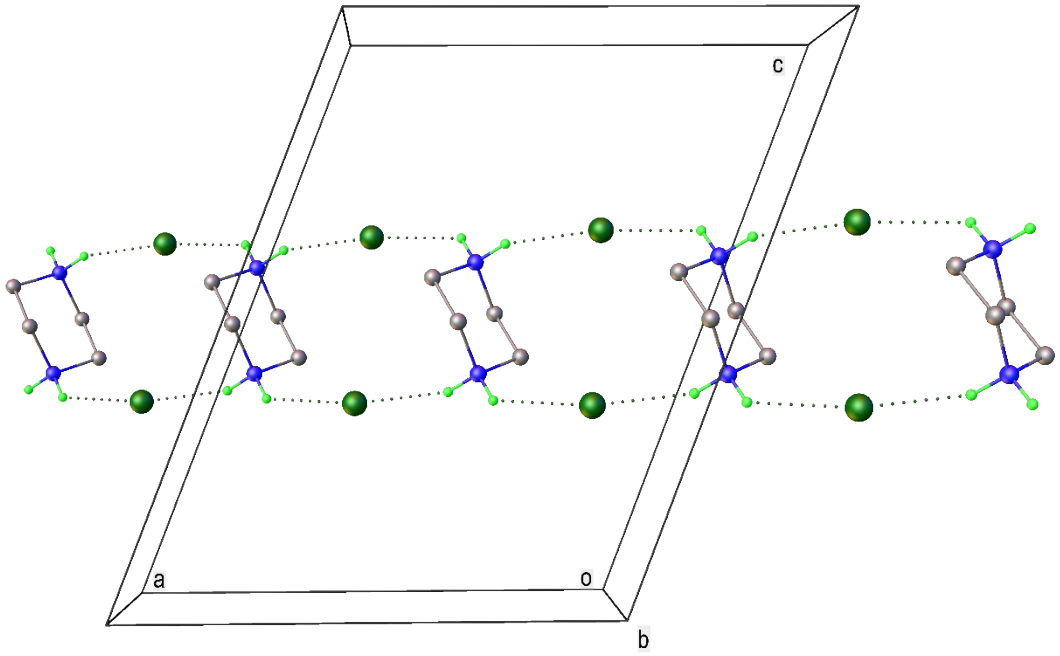

Figure S14. Hydrogen-bonded chains in 6 parallel to ab diagonal. H atoms of alkyl fragments are omitted for clarity. Hydrogen bonds are shown by dashed lines.

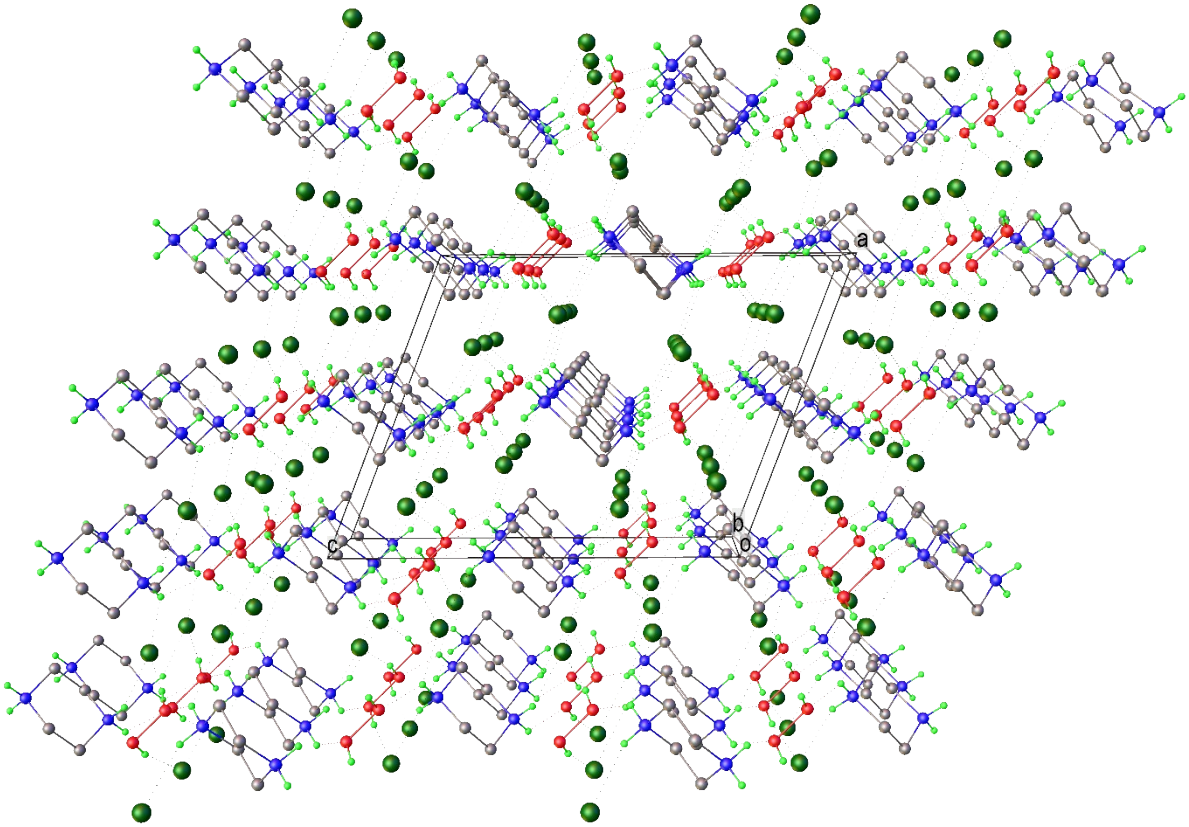

Figure S15. Crystal packing in 6. H atoms of alkyl fragments are omitted for clarity. Hydrogen bonds are shown by dashed lines.

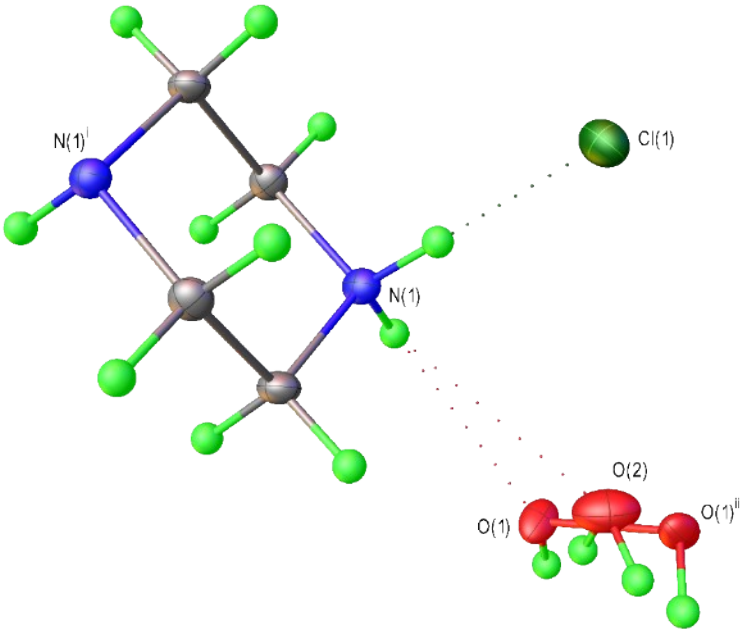

Figure S16. Asymmetric unit in structures **7** and **8**. Displacement ellipsoids are shown at the 50% probability level. Hydrogen bonds are shown by dashed lines. Symmetry codes: (i) 1-x, 2-y, 1-z; (ii) 1-x, +y, 3/2-z.

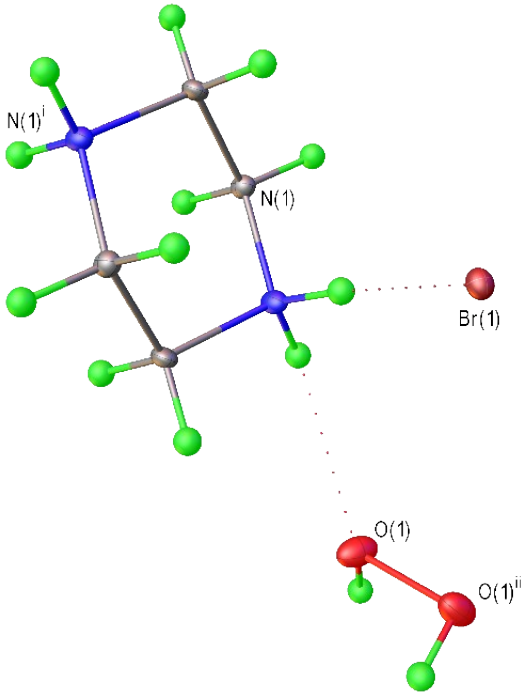

Figure S17. Asymmetric unit in structure **9**. Displacement ellipsoids are shown at the 50% probability level. Hydrogen bonds are shown by dashed lines. Symmetry codes: (i) 1-x, 1-y, 1-z; (ii) 1-x, +y, 1/2-z.

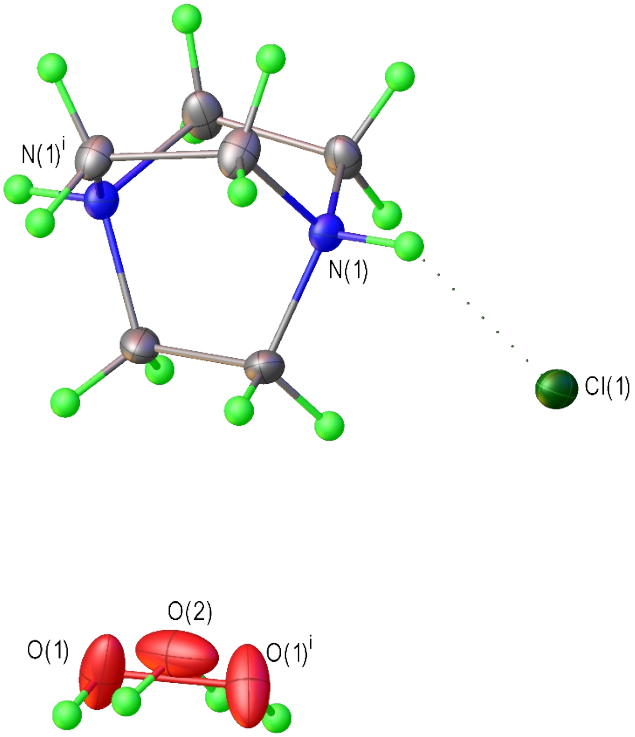

Figure S18. Asymmetric unit in structure **11**. Displacement ellipsoids are shown at the 50% probability level. Hydrogen bonds are shown by dashed lines. Symmetry code: (i) 1-x, y, 3/2-z.

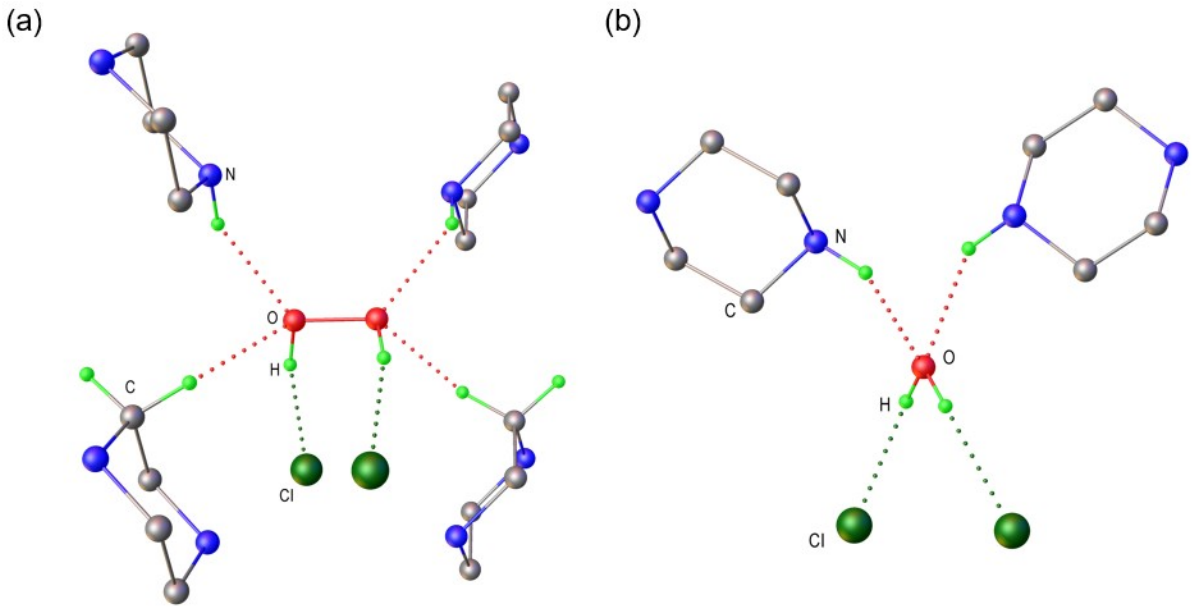

Figure S19. Hydrogen bonding of hydrogen peroxide and water molecules in the optimized structures of **8**-H_2O_2 (a) and **8**-H_2O (b), respectively. H atoms of alkyl fragments are omitted for clarity. Hydrogen bonds are shown by dashed lines.

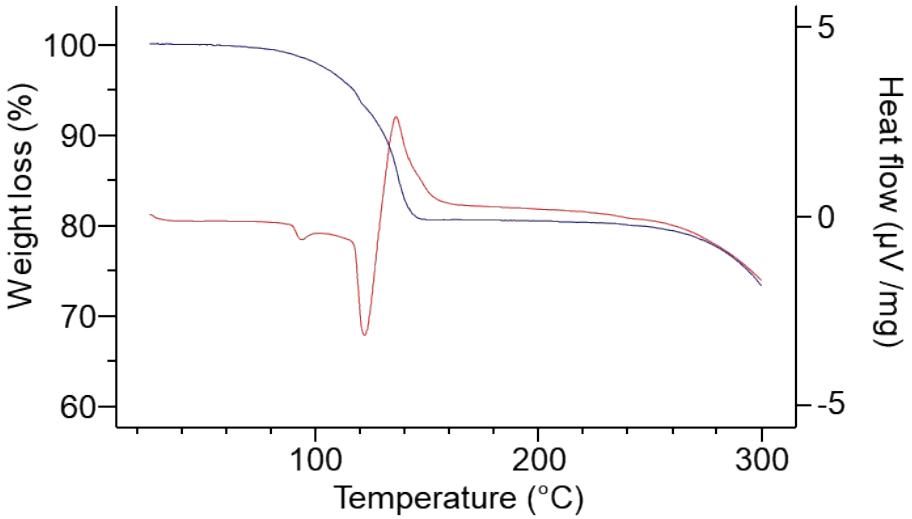

Figure S20. TG (blue) and DTA (red) curves of ethylenediammonium dichloride peroxosolvate **3**.

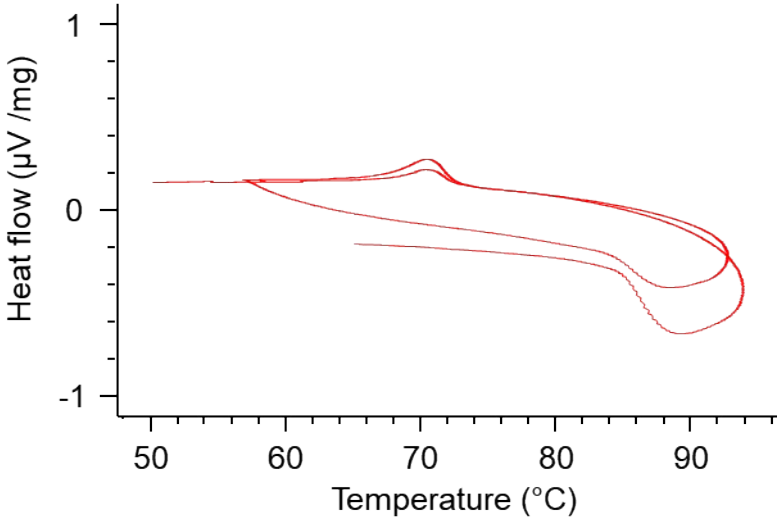

Figure S21. DTA cycling of **3** showing the reversible melting and crystallization of peroxosolvate.

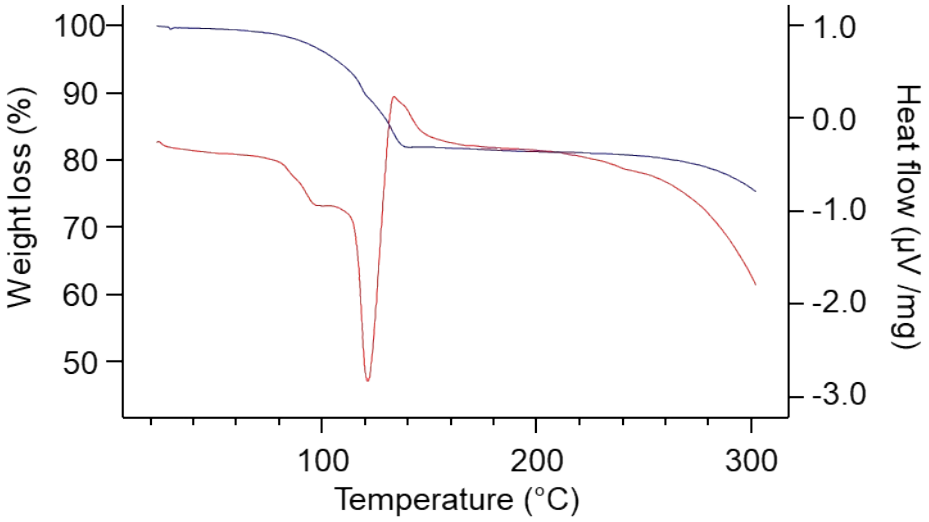

Figure S22. TG (blue) and DTA (red) curves of ethylenediammonium dichloride partially hydrated peroxosolvate **4**.

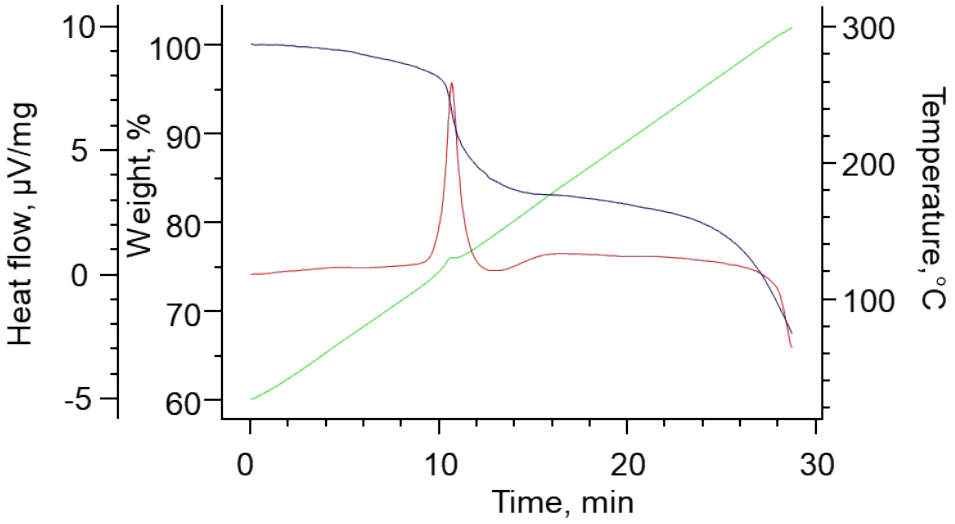

Figure S23. TG (blue) and DTA (red) curves of piperazinium dichloride monoperoxosolvate obtained from 5% w/w H_2O_2 (**8**).

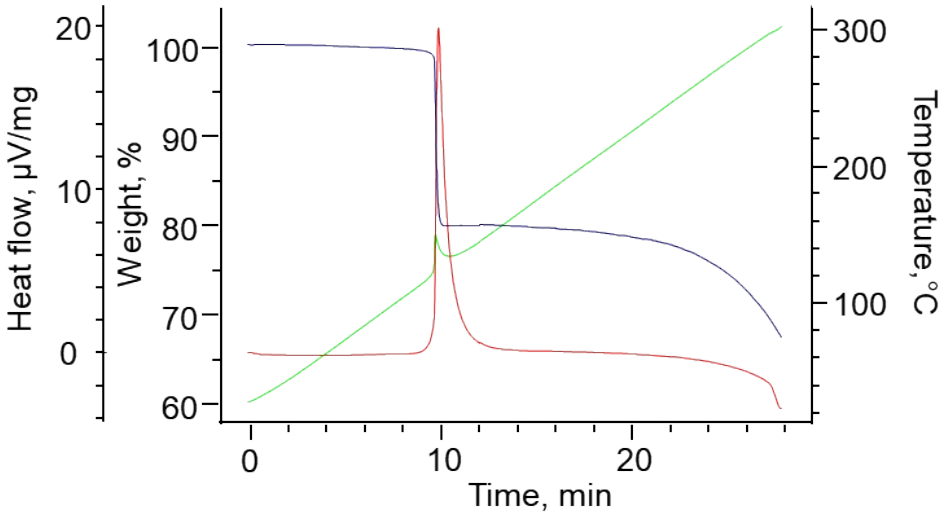

Figure S24. TG (blue) and DTA (red) curves of piperazinium dichloride monoperoxosolvate obtained from 20% w/w H_2O_2.

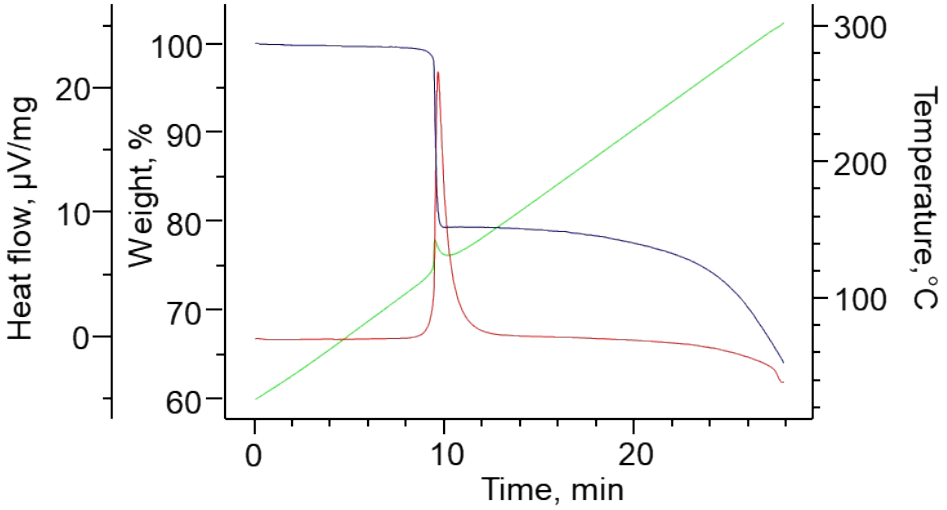

Figure S25. TG (blue) and DTA (red) curves of piperazinium dichloride monoperoxosolvate obtained from 50% w/w H_2O_2 (**6**).

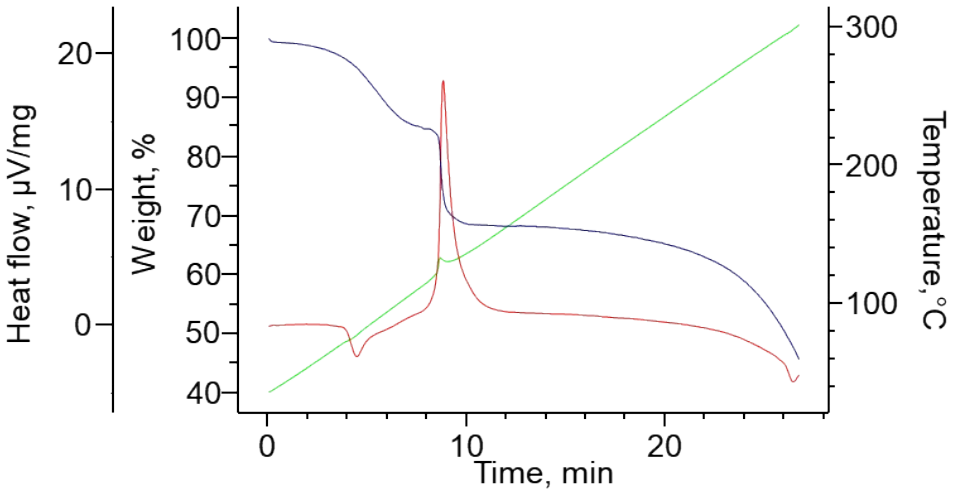

Figure S26. TG (blue) and DTA (red) curves of piperazinium dichloride diperoxosolvate obtained from 97% w/w H_2O_2 (**5**).

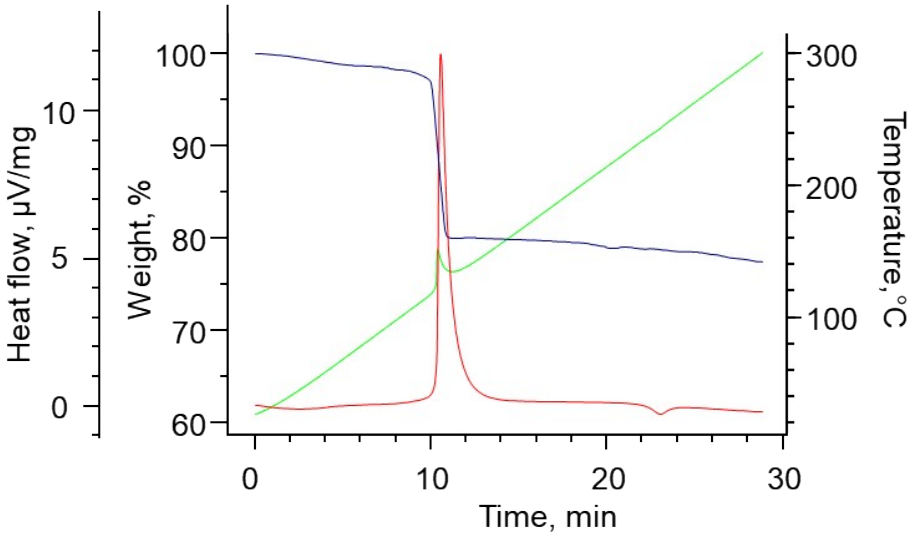

Figure S27. TG (blue) and DTA (red) curves of piperazinium dibromide monoperoxosolvate obtained from 50% w/w H_2O_2 (**9**).

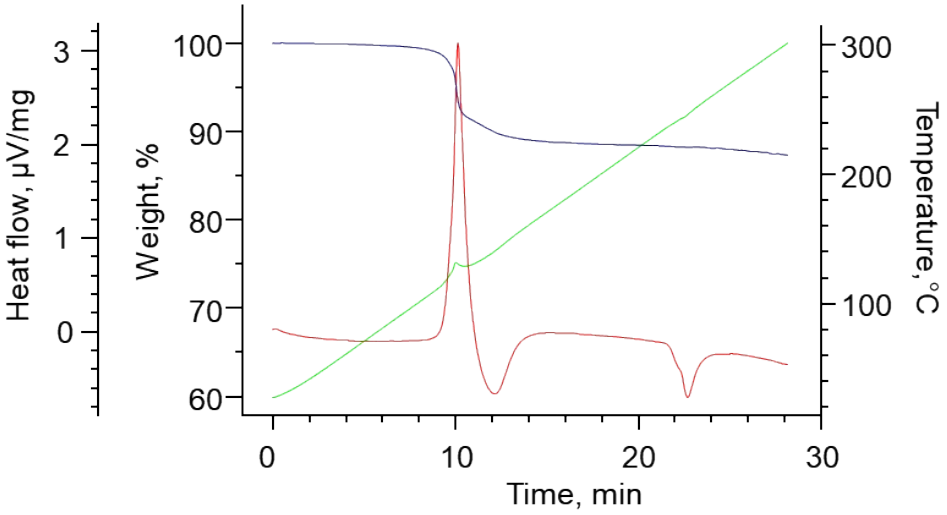

Figure S28. TG (blue) and DTA (red) curves of piperazinium dibromide monoperoxosolvate obtained from 10% w/w H_2O_2.

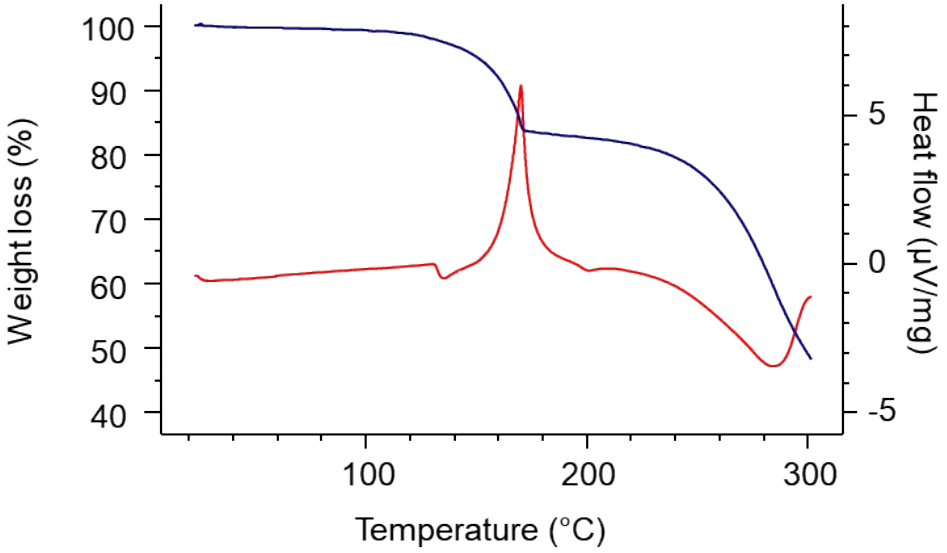

Figure S29. TG (blue) and DTA (red) curves of triethylenediaminium dichloride peroxosolvate **10**.

References

(1) Maass, O.; Hatcher, W. H. The properties of pure hydrogen peroxide. I. *J. Am. Chem. Soc.* **1920**, *42* (12), 2548–2569. https://doi.org/10.1021/ja01457a013.

(2) Schumb, W. C.; Satterfield, C. N.; Wentworth, R. L. *Hydrogen Peroxide*; Reinhold Publishing Corporation: New York, 1955. https://doi.org/10.1002/jps.3030450224.

(3) Mikhaylov, A. A.; Medvedev, A. G.; Egorov, P. A.; Mayorov, N. S.; Zhizhin, K. Y.; Prikhodchenko, P. V. Laboratory Method for Obtaining Anhydrous Hydrogen Peroxide and Safety Rules for Handling It. *Russ. J. Gen. Chem.* **2024**, *94* (12), 3333–3339. https://doi.org/10.1134/S1070363224120235.

(4) Sivaraj, S.; Vijayamathubalan, P.; Chidambaranathan, B.; Gunaseelan, R.; Sagayaraj, P.; Selvakumar, S. Piperazinium Dibromide Monohydrate (PDBM) Third-Order NLO Single Crystal: Analysis on Structural, Optical, Thermal, Electrical and Mechanical Properties. *J Mol. Struct.* **2025**, *1324*, 140705. https://doi.org/10.1016/J.MOLSTRUC.2024.140705.

(5) Kennedy, S. W.; Schultz, P. K.; Slade, P. G.; Tiekink, E. R. T. Triethylenediamine Dihydrochloride. *Z. Kristallogr. – Cryst. Mater.* **1987**, *180* (1–4), 211–218. https://doi.org/10.1524/zkri.1987.180.14.211.

(6) Sheldrick, G. M. SADABS, Programs for Scaling and Absorption Correction of Area Detector Data. *SADABS ver. 2016/2 - Bruker AXS area detector scaling and absorption correction program* **2016**, Bruker AXS, Karlsruhe, Germany.

(7) Sheldrick, G. M. Crystal Structure Refinement with SHELXL. *Acta Crystallogr., Sect. C: Struct. Chem.* **2015**, *71*, 3–8. https://doi.org/10.1107/S2053229614024218.

(8) Erba, A.; Desmarais, J. K.; Casassa, S.; Civalleri, B.; Donà, L.; Bush, I. J.; Searle, B.; Maschio, L.; Edith-Daga, L.; Cossard, A.; Ribaldone, C.; Ascrizzi, E.; Marana, N. L.; Flament, J.-P.; Kirtman, B. CRYSTAL23: A Program for Computational Solid State Physics and Chemistry. *J. Chem. Theory Comput.* **2023**, *19* (20), 6891–6932. https://doi.org/10.1021/acs.jctc.2c00958.

(9) Cossard, A.; Desmarais, J. K.; Casassa, S.; Gatti, C.; Erba, A. Charge Density Analysis of Actinide Compounds from the Quantum Theory of Atoms in Molecules and Crystals. *J. Phys. Chem. Lett.* **2021**, *12* (7), 1862–1868. https://doi.org/10.1021/acs.jpclett.1c00100.

(10) Mata, I.; Alkorta, I.; Espinosa, E.; Molins, E. Relationships between Interaction Energy, Intermolecular Distance and Electron Density Properties in Hydrogen Bonded Complexes under External Electric Fields. *Chem. Phys. Lett.* **2011**, *507* (1–3), 185–189. https://doi.org/10.1016/j.cplett.2011.03.055.

(11) Bader, R. F. W. A Quantum Theory of Molecular Structure and Its Applications. *Chem. Rev.* **1991**, *91* (5), 893–928. https://doi.org/10.1021/cr00005a013.

(12) Medvedev, A. G.; Churakov, A. V.; Prikhodchenko, P. V.; Lev, O.; Vener, M. V. Crystalline Peroxosolvates: Nature of the Coformer, Hydrogen-Bonded Networks and Clusters, Intermolecular Interactions. *Molecules* **2021**, *26* (1), 26. https://doi.org/10.3390/molecules26010026.

(13) Navasardyan, M. A.; Bezzubov, S. I.; Medvedev, A. G.; Prikhodchenko, P. V.; Churakov, A. V. Novel Peroxosolvates of Tetraalkylammonium Halides: The First Case of Layers

Containing Hydrogen-Bonded Peroxide Molecules. *CrystEngComm* **2022**, *24* (1), 38–42. https://doi.org/10.1039/D1CE01476E.

(14) Churakov, A. V.; Prikhodchenko, P. V.; Howard, J. A. K. The Preparation and Crystal Structures of Novel Perhydrates Ph4X+Hal–·nH2O2: Anionic Hydrogen-Bonded Chains Containing Hydrogen Peroxide. *CrystEngComm* **2005**, *7* (110), 664. https://doi.org/10.1039/b511834d.

(15) Infantes, L.; Chisholm, J.; Motherwell, S. Extended Motifs from Water and Chemical Functional Groups in Organic Molecular Crystals. *CrystEngComm* **2003**, *5* (85), 480–486. https://doi.org/10.1039/B312846F.

(16) Grishanov, D. A.; Navasardyan, M. A.; Medvedev, A. G.; Lev, O.; Prikhodchenko, P. V.; Churakov, A. V. Hydrogen Peroxide Insular Dodecameric and Pentameric Clusters in Peroxosolvate Structures. *Angew. Chem., Int. Ed.* **2017**, *56* (48), 15241–15245. https://doi.org/10.1002/anie.201709699.

(17) Chohan, S.; Pritchard, R. G. Tripotassium Tris(Oxalato-κ 2 O , O ′)Aluminate Bis(Hydrogen Peroxide) Hydrate, the First Example of a Cyclic Hydrogen-Bonded H 2 O 2 Dimer. *Acta. Crystallogr., Sect. C* **2003**, *59* (5), m187–m189. https://doi.org/10.1107/S0108270103006905.

(18) Hinrichs, F.; Adam, A. Ein Neues Salz Der Monoperoxokohlensäure: K2(O2)CO2·3.5H2O2. *Z. Anorg. Allg. Chem.* **2011**, *637* (3–4), 426–429. https://doi.org/10.1002/zaac.201000322.

(19) Ahn, S. H.; Cluff, K. J.; Bhuvanesh, N.; Blümel, J. Hydrogen Peroxide and Di(Hydroperoxy)Propane Adducts of Phosphine Oxides as Stoichiometric and Soluble Oxidizing Agents. *Angew. Chem., Int. Ed.* **2015**, *54* (45), 13341–13345. https://doi.org/10.1002/anie.201505291.

(20) Chernyshov, I. Y.; Vener, M. V.; Prikhodchenko, P. V.; Medvedev, A. G.; Lev, O.; Churakov, A. V. Peroxosolvates: Formation Criteria, H 2 O 2 Hydrogen Bonding, and Isomorphism with the Corresponding Hydrates. *Cryst. Growth Des.* **2017**, *17* (1), 214–220. https://doi.org/10.1021/acs.cgd.6b01449.

(21) Prikhodchenko, P. V.; Medvedev, A. G.; Tripol'skaya, T. A.; Churakov, A. V.; Wolanov, Y.; Howard, J. A. K.; Lev, O. Crystal Structures of Natural Amino Acid Perhydrates. *CrystEngComm* **2011**, *13* (7), 2399. https://doi.org/10.1039/c0ce00481b.